Development 128, 4153-4164 (2001)
Printed in Great Britain © The Company of Biologists Limited 2001
DEV1653

Fgf signalling through MAPK cascade is required for development of the subpallial telencephalon in zebrafish embryos

Minori Shinya[1,2], Sumito Koshida[3], Atsushi Sawada[1,2], Atsushi Kuroiwa[1] and Hiroyuki Takeda[2,*,‡]

[1]Division of Biological Science, Graduate School of Science, Nagoya University, Chikusa-ku, Nagoya, 464-8602 Japan
[2]Early Embryogenesis, Department of Developmental Genetics, National Institute of Genetics, Yata 1111, Mishima, 411-8540 Japan
[3]Kondoh Differentiation Signalling Project ERATO, JST, Kinkichihou Hatsumei Centre, 14 Kawaramachi, Yoshida, Sakyo-ku, Kyoto, 606-8305 Japan
*Department of Biological Sciences, Graduate School of Science, University of Tokyo, Hongo 7-3-1, Bunkyo-ku, Tokyo 113-0033, Japan
‡Author for correspondence (e-mail: htakeda@biol.s.u-tokyo.ac.jp)

Accepted 8 August 2001

SUMMARY

The telencephalon is formed in the most anterior part of the central nervous system (CNS) and is organised into ventral subpallial and dorsal pallial domains. In mice, it has been demonstrated that Fgf signalling has an important role in induction and patterning of the telencephalon. However, the precise role of Fgf signalling is still unclear, owing to overlapping functions of Fgf family genes. To address this, we have examined, in zebrafish embryos, the activation of Ras/mitogen-activated protein kinase (MAPK), one of the major downstream targets of Fgf signalling. Immunohistochemical analysis reveals that an extracellular signal-regulated kinase (ERK), a vertebrate MAPK is activated in the anterior neural boundary (ANB) of the developing CNS at early segmentation stages. Experiments with Fgf inhibitors reveal that ERK activation at this stage is totally dependent on Fgf signalling. Interestingly, a substantial amount of ERK activation is observed in *ace* mutants in which *fgf8* gene is mutated. We then examine the function of Fgf signalling in telencephalic development by use of several inhibitors to Fgf signalling cascade, including dominant-negative forms of Ras (Ras^{N17}) and the Fgf receptor (Fgfr), and a chemical inhibitor of Fgfr, SU5402. In treated embryos, the induction of telencephalic territory normally proceeded but the development of the subpallial telencephalon was suppressed, indicating that Fgf signalling is required for the regionalisation within the telencephalon. Finally, antisense experiments with morpholino-modified oligonucleotides suggest that zebrafish *fgf3*, which is also expressed in the ANB, co-operates with *fgf8* in subpallial development.

Key words: *fgf3*, Ras, ERK, morpholino, SU5402, regionalisation, Zebrafish

INTRODUCTION

The telencephalon is the anterior-most structure in the CNS. Though its morphologies are quite divergent in different species, organisation of telencephalic subdivisions, subpallial and pallial territories, are basically conserved between species (Wilson and Rubenstein, 2000). The subpallial telencephalon constitutes most of the basal ganglia and the pallial telencephalon contains the progenitors in the cerebral cortex in mammals. Fate-mapping studies have revealed that the telencephalon derives from cells at the anterior margin of the neural plate (Rubenstein et al., 1998; Whitlock and Westerfield, 2000). Experiments with mice and zebrafish have demonstrated that the tissue located in the ANB plays an important role in induction and patterning of the telencephalic region (Shimamura and Rubenstein, 1997; Houart et al., 1998). Fgf8 expressed in the ANB has been implicated in these processes (Shimamura and Rubenstein, 1997; Reifers et al., 1998; Shanmugalingam et al., 2000). The phenotypes of zebrafish *ace* mutants, in which no functional Fgf8 is produced, reveal the function of *fgf8* in the regionalisation of the telencephalon; some subpallial markers are downregulated in the mutants (Reifers et al., 1998; Shanmugalingam et al., 2000). Furthermore, mutant mice in which *fgf8* function is reduced, show the loss of olfactory bulb and reduction of the forebrain (Meyers et al., 1998). However, owing to overlapping expression and functional redundancy of Fgf family genes (Maruoka et al., 1998; Xu et al., 1999), a precise role of Fgf signalling in development of the telencephalon remains unclear.

We address this question in zebrafish embryos by direct observation of the response to Fgfs. Fgf receptors are members of the receptor tyrosine kinase (RTK) superfamily (Klint and Claesson-Welsh, 1999; Ornitz, 2000). At present, four members are known and each of them has several splicing isoforms (Klint and Claesson-Welsh, 1999). In general, RTKs trigger, by way of Ras, a sequential activation of the mitogen-activated protein kinase (MAPK) (or extracellular regulated

kinase (ERK)) signalling cascade (Cobb and Goldsmith, 1995). ERK is activated by dual phosphorylation of threonine and tyrosine residues by MAPK/ERK kinase (MEK) (Crews et al., 1992). A monoclonal antibody raised against a dually phosphorylated form of ERK (dpERK) has been successfully applied to *Drosophila* and *Xenopus*, and reveals a dynamic dpERK staining pattern in early embryos (Gabay et al., 1997a; Gabay et al., 1997b; Christen and Slack, 1999). In *Drosophila*, several different RTKs participate in ERK activation, while, in *Xenopus*, the Fgf family seems to be responsible for the full pattern of dpERK in early development as activation can be blocked by the expression of a dominant-negative form of Fgf receptor (Christen and Slack, 1999).

We find that ERK is activated in the zebrafish ANB. Like *Xenopus*, the activation in the ANB is attributable to an Fgf signal. Interestingly, ERK activation in the ANB is maintained in *ace* mutants, suggesting other Fgfs function in this region. We also examined the function of Fgf signalling in zebrafish forebrain patterning by use of several inhibitors of the Fgf/Ras/MAPK signalling cascade, such as dominant-negative form of Ras (Ras^{N17}) and the Fgf receptor, and a chemical inhibitor of Fgfr, SU5402. In treated embryos, the induction of telencephalic territory proceeds normally but the development of the subpallial telencephalon is suppressed, indicating that Fgf signalling is required for the regionalisation within the telencephalon. Finally, we show using antisense that both Fgf3 and Fgf8 are required for normal development of the subpallial region.

MATERIALS AND METHODS

Fish maintenance

Zebrafish, *Danio rerio*, were maintained at 26°C and embryos were collected from natural crosses of wild-type fish. Homozygotes of ace^{ti282a} were obtained from crosses of heterozygotes. Collected embryos were maintained in 1/3 Ringer's solution (39 mM NaCl, 0.97 mM KCl, 1.8 mM $CaCl_2$, 1.7 mM Hepes at pH 7.2) at 28.5°C. Embryos were staged according to hours postfertilisation (hpf) at 28.5°C and morphological criteria (Kimmel et al., 1995).

mRNA and morpholino injection

Capped sense RNAs were synthesised using the mMESSAGE mMACHINE™ large scale in vitro transcription kit (Ambion) from the plasmid containing full-length human Ras^{N17} (Deng and Karin, 1994), *Xenopus bΔFR4* (Hongo et al., 1999), and zebrafish *fgf3*, *fgf3-myc*, *GFP* and *lacZ*. *GFP* and *lacZ* RNA were used as a control. The mRNAs were diluted to 0.8-1.0 μg/μl with distilled water and 200-500 ng/μl (Ras^{N17}), 400 ng/μl (*bΔFR4*), 5 ng/μl (*fgf3-myc*) or/and 5 or 100 ng/μl (*fgf3*) mRNAs were injected into one- to two-cell stage embryos. Morpholino oligonucleotides were solubilised in water at the concentration of 50 μg/μl. The resulting stock solution was diluted to working concentrations in water before injection into one- to two-cell stage embryos. Injected embryos were cultured in 1/3 Ringer's solution until use. The sequences of morpholino oligonucleotides used in the present study were as follows (see Fig. 9N): fgf8-MO, 5′-TCAACCGTGAAGGTATGAGTCTC-3′; fgf3-MO, 5′-TATAA-CCATTGTGGCATGGCGGGAT-3′; 4-mis-MO, 5′-TATTACCTTT-GTGGCATGCCGGCAT-3′; and fgf3-MO', 5′-CAACAAGAGCAG-AATTATAACCATT-3′.

For construction of *fgf3-myc*, the full-length of *fgf3* cDNA was amplified by PCR and inserted into pCS2+ containing 6× Myc epitopes such that the Myc epitope is placed in the C terminus of Fgf3 (kindly provided by Dr M. Hibi, Osaka University).

Beads transplantation and SU5402 treatment

Mouse recombinant Fgf8b protein (R&D Systems) or BSA was used at the concentration of 0.25 μg/μl. Preparation of the beads soaked in Fgf8b or BSA were performed as described in Makita et al. (Makita et al., 1998). Dechorionated embryos at tailbud stage were placed in 3% methylcellulose in 1/3 Ringer's solution and transplanted into the forebrain using a tungsten needle. After transplantation, embryos were cultured at 28.5°C in 1/3 Ringer's solution until use.

For injection, 10 mg/ml SU5402 (Calbiochem) in DMSO was used. Dechorionated embryos were placed in 1.5% methylcellulose in 1/3 Ringer's solution and injected into thick head region at tailbud stage. DMSO was injected as a control. Alternatively, dechorionated embryos at proper stages were soaked for 10 minutes in SU5402/1/3 Ringer solution at a concentration of 0.1 mg/ml, and washed several times with 1/3 Ringer's solution. Treated embryos were cultured at 28.5°C in 1/3 Ringer's solution until use. We found that the activity of SU5402 varied a great deal, depending on the lot number. Thus, the incubation was sometimes carried out at a concentration of 0.2 mg/ml.

Detection of apoptosis

Apoptosis in zebrafish whole-mounts was detected according to a protocol given by the manufacturer with some modifications (Dead End™ Colorimetric Apoptosis Detection System, Promega). After fixation overnight in 4% paraformaldehyde (PFA) in phosphate-buffered saline (PBS), embryos were transferred in methanol and then rehydrated in PBST (PBS/0.1% Tween 20). Subsequently, embryos were digested in 5 μg/ml proteinase K in PBS for 5 minutes and postfixed for 20 minutes in 4% PFA in PBS. Then the embryos were immersed in acetone for 7 minutes at –20°C and incubated in the equilibration buffer (provided in the kit) for 10 minutes at the room temperature. After incubation for 3 hours at 37°C in working strength terminal deoxynucleotidyl transferase (TdT) enzyme, the DNA end-labelling reaction using biotinylated dUTP was stopped by washing in 2× saline sodium citrate (SSC) and PBST. Biotin was detected by horseradish-peroxidase-labelled streptavidin with diaminobenzidine (DAB).

Whole-mount in situ hybridisation and histological analysis

Digoxigenin-labelled probes were synthesised by in vitro transcription using T3, T7 and SP6 polymerases. Whole-mount in situ hybridisation was performed by the standard protocol with some modifications (Schulte-Merker et al., 1992).

For histological analysis, the specimens were embedded in Technovit 8100 (Heraeus Kulzer, Wehrheim) and cut at 7 μm.

Immunohistochemistry and western blot

For whole-mount immunostaining, embryos were fixed with 3.7% formaldehyde/0.2% glutaraldehyde/PBS for 1 hour at room temperature. After washing with PBS, they were dehydrated with methanol and transferred to PBS. Then, they were washed with MABT (MAB/0.1% TritonX-100; MAB, 100mM maleic acid and 150 mM NaCl) three times for 10 minutes and MABDT (MAB/0.1% Triton X-100/1% DMSO) twice for 30 minutes. After blocking with 2% FCS/MABDT, the embryos were incubated in the blocking solution containing 1:10000 anti-di-phosphorylated ERK1 and ERK2 (MAPK-YT) antibody (Sigma) for overnight at 4°C. They were then washed with MABDT three times for 5 minutes, four times for 30 minutes, and incubated in blocking solution again for 30 minute, followed by incubation with the second antibody (1:500 anti-mouse IgG biotin conjugated antibody, Vector Laboratory) for 2 hours at room temperature. After the washing with MABDT as described above, the signals were detected with ABC staining kit according to the manufacturer's instructions (Vector Laboratory). To examine ERK activation in *ace* homozygous mutants at the five-somite stage, embryos obtained from two heterozygous *ace* carriers were cut into

two pieces at the level of the hindbrain, and they were fixed immediately. The anterior and posterior halves were then processed for dpERK or myoD staining, respectively.

Western blot analysis was performed following the standard method for ECL western blotting detection reagent (Amersham Pharmacia Biotech). Proteins from three embryos were separated by 12.5% polyacrylamide gels and transferred to Hybond^{TM} ECL^{TM} membranes (Amersham Pharmacia Biotech) by electroblotting. Monoclonal antibody against dpERK was used at the same concentration as used in immunostaining. The homogenates were prepared from whole embryos at 75% epiboly, bud and the six- to seven-somite stage. *ace* homozygotes could be distinguished by morphology by the six-somite stage.

For detection of Fgf3-Myc, 15 blastoderms taken from sphere-stage embryos injected with RNAs were loaded in each lane. The same staining protocol was applied except for that 9E10 (1:100 dilution, kindly provided by Dr Tatsumi Hirata, National Institute of Genetics) and 2% skim milk were used as the first antibody and as a blocking solution, respectively.

BrdU labelling and detection

To analyse cell mitosis at early segmentation stages, about 0.5 nl of 25 mM of BrdU (SIGMA) was injected into the yolk at tailbud stage. After 3 hours' incubation, injected embryos were fixed with 4% PFA/PBS for 2 hours at room temperature. After washing with PBS, the embryos were dehydrated with 25%, 75% and 100% methanol, and rehydrates in PBST. They were then treated with proteinase K (5 μg/ml in PBS) for 5 minutes at 37°C and with glycine-HCl (2mg/ml, pH 2.2) for 5 minutes at room temperature, followed by washing with PBST and post-fixation with 4%PFA/PBS for 20 minutes at room temperature. After washing with PBST, the embryos were treated with 2N HCl for 20 minutes at room temperature to relax chromatin and facilitate immunodetection of incorporated BrdU. Acid-treated embryos were then washed in PBSDT (1%DMSO, 0.1%Tween20 in PBS), incubated with PBSDNT (PBSDT+2% foetal calf serum) for 30 minutes at room temperature, followed by overnight incubation with anti-BrdU antibody (1:200 dilution in PBSDNT, Sigma) at 4°C. After intense washing with PBSDT and blocking with PBSDNT, the embryos were incubated overnight with the second antibody (1:500 dilution in PBADNT, anti-mouse IgG antibody biotin-conjugated, Vector Laboratory) at 4°C. After intense washing in PBSDT, the signals were detected with ABC staining kit as described above.

For cell count, the stained embryos were embedded in Technovit 8100 and serially sectioned at 5 μm. Three sagittal sections (more than 10 μm apart to each other) at the midline of the telencephalon from each treated embryo were selected, and the total number of positive and negative cells in each section was counted (six to seven embryos for each treatment). The 'ventral' corresponds approximately to the region that is positive for ERK staining.

RESULTS

ERK activation pattern in developing embryos

ERK is one of well-known downstream mediators of Fgf receptor (Gotoh and Nishida, 1996; Chirsten and Slack, 1999). We examined the pattern of ERK activation in whole embryos, focusing on the anterior neural region. During gastrulation, strong activation is detected in the blastoderm margin that gives rise to the mesoderm (Fig. 1A). This activation is finally confined to the tailbud region by the end of gastrulation. The midbrain/hindbrain boundary (MHB) becomes positive at the end of gastrulation, and the activation reaches a peak level at the three-somite stage (Fig. 1B). After the activation in the MHB, the anterior part of the forebrain becomes positive at the three-somite stage, and the strongest staining is observed at the five-somite stage (asterisk in Fig. 1C). Histological sections of the five-somite stage embryos reveal that ERK activation in the forebrain is confined to the ANB (Fig. 1D). The activation gradually decrease (Fig. 1E,F), and become undetectable by the stages later than 12 somites. The activated pattern closely resembles that reported in *Xenopus* (Christen and Slack, 1999).

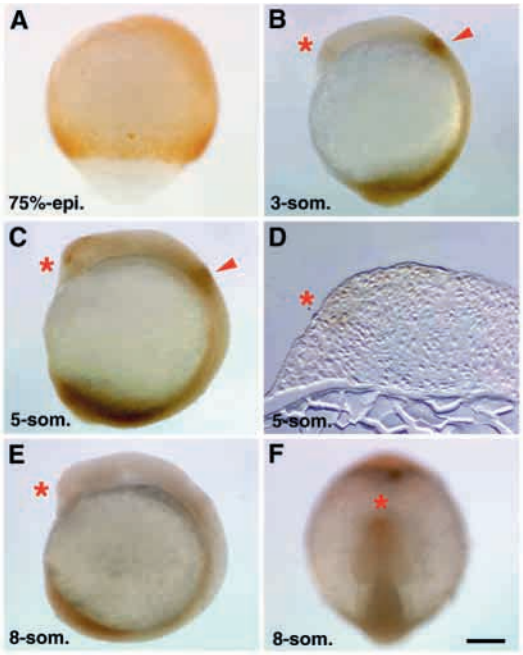

Fig. 1. ERK activation detected by anti-dpERK antibody in wild-type embryos. (A-C,E) Lateral view, dorsal towards the right. (F) Dorsal view of the head region. (A) 75% epiboly stage; ERK activation is seen in the marginal mesoderm. (B) Three-somite stage; ERK activation is seen in the MHB and tailbud, and weakly in the ANB. (C) Five-somite stage; ERK activation in the ANB becomes strong. (D) Sagittal section of the embryo shown in C. ERK is strongly activated in the ANB (C,D). (E,F) Eight-somite stage; staining in the ANB is faint. Asterisks indicate the staining in the ANB and arrowheads indicate the staining in the MHB. Scale bar: 100 μm in A-C,E,F; 30 μm in D.

Fgf-dependent activation of ERK at segmentation stages

As ERK activation is triggered by downstream targets of various RTKs (see Introduction), we examined the contribution of Fgf signalling toward ERK activation by use of inhibitors to Fgf signalling cascade. We first tested whether or not ERK activation at segmentation stages is Ras-dependent by injecting synthetic RNAs encoding dominant-negative form of human Ras (Ras^{N17}), in which serine at position 17 had been substituted by asparagine (Deng and Karin, 1994). The synthetic RNAs were injected at one- to two-cell stages, and stained for dpERK at segmentation stages. In Ras^{N17}-injected embryos, all positive staining disappeared (43/48, Fig. 2A,B). We then examined the effects of XFD (Amaya et al., 1991) and bΔFR4 (Hongo et al., 1999), a dominant-negative form of *Xenopus* Fgfr1 and Fgfr4a, respectively. Both types of dominant-negative Fgfrs effectively reduced ERK staining (24/24 for XFD and 30/30 for bΔFR4; Fig. 2C), although the

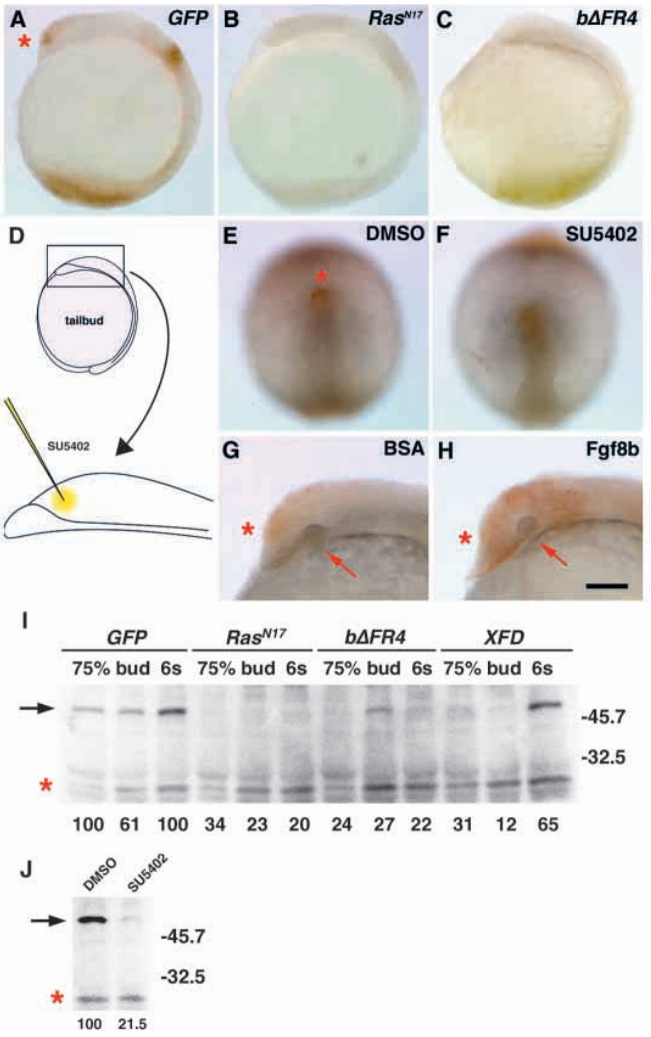

Fig. 2. ERK activation in embryos treated with inhibitors to Fgf signalling. All embryos were analysed at the five-somite stage. (A-C) Lateral view, dorsal towards the right; ERK activation observed in *GFP*-injected embryo (A) is suppressed by injection of *Ras*^{N17} (B) and *bΔFR4* (C) RNAs. (D) Schematic representation of the SU5402 injection; SU5402 (F) or DMSO as a control (E) was injected into the head region at the tailbud stage. (E,F) Dorsal view of the head region; ERK activation in the ANB is suppressed by the injection of SU5402 (F). (G,H) Lateral view of the head region; BSA- (G) or Fgf8b- (H) soaked beads were transplanted in the thick head region at tailbud stage. Ectopic ERK activation is found around the Fgf8b beads (H). (I) Western blot analysis of activated ERK after RNA injections. Homogenates prepared from injected embryos at 75% epiboly, tailbud (bud) and six-somite (6s) stages are loaded. Western blot detects one major band of about 50 kDa (arrow), which is sensitive to inhibitor injections. Relative intensity of the major band is shown at the bottom of each lane. (J) Western blot analysis of activated ERK after SU5402 treatment (soak method, see Fig. 8E,F). Homogenates prepared from control- and SU5402-treated embryos at the three-somite stage are loaded. Relative intensity of the major band is shown at the bottom of each lane. Relative intensities in (I,J) were normalised by a nonspecific minor band (asterisk) that is insensitive to any treatments. Asterisks in A-H indicate endogenous staining in the ANB and arrows indicate the transplanted beads. Scale bar: 100 μm in A-F; 50 μm in G,H.

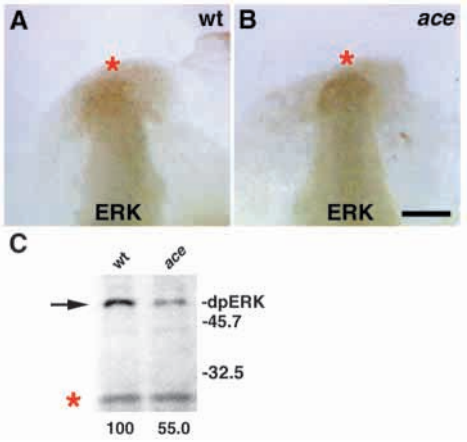

Fig. 3. Immunostaining and western blot for activated ERK in *ace* mutants. (A,B) Dorsal views of the head region at the five-somite embryos stained with anti-dpERK antibody. ERK activation in the ANB is detected in both the wild-type (A) and *ace* homozygous mutant (B). Asterisks indicate the anterior edge of the neural plate. (C) Western blot analysis of activated ERK; the equal amount of homogenates prepared from wild-type and *ace* mutant at the six- to seven-somite stage were loaded in each lane. Relative intensity of the major band is shown at the bottom of each lane. Relative intensity was normalised by a non-specific minor band (asterisk) that is insensitive to any Fgf inhibitors (see Fig. 2). Scale bar: 50 μm in A,B.

effect of XFD tended to be weak. Finally, developing embryos were treated with a chemical inhibitor to Fgfr, SU5402. SU5402 has been reported to inhibit specifically the kinase activity of nearly all types of Fgfr (Mohammadi et al., 1997). We injected 10 mg/ml of SU5402 into the anterior thick region of the brain near the ANB at tailbud stage (see Fig. 2D), and the embryos were fixed at the five-somite stage, followed by anti-dpERK staining. Again, the positive staining in the ANB was greatly reduced in injected embryos (19/19, Fig. 2E,F). Western blot analysis confirmed this result. As shown in Fig. 2I,J, one major band (50 kDa) was detected by anti-dpERK antibody. The intensity of this band much decreased (about 20% of the control) after injection of *Ras*^{N17} or *bΔFR4* RNAs and SU5402 treatment (Fig. 2I,J). However, the effect of *XFD* RNAs did not last long, and the activation level recovered to more than 50% by the six-somite stage (Fig. 2I).

Fgf-dependent activation of ERK was further examined by transplantation of Fgf-soaked beads into the anterior head region. Ectopic activation of ERK was induced around the transplanted beads that had been soaked in PBS containing recombinant mouse Fgf8b (15/15, Fig. 2H), while no such activation was detected around BSA-soaked bead (12/13, Fig. 2G). Taken together, we conclude that under our experimental conditions, ERK activation in the ANB was entirely dependent on Fgf signalling. Though ERK activation may not represent all the activity of Fgf signalling, it is reasonable to assume that the positive staining is an indicator for the activation of Fgf signalling.

ERK is activated in the ANB of *ace* mutants

We then examined ERK activation in *ace* mutants. The *ace* mutation is a G to A transition in the splice site after the second exon of the *fgf8* gene, which leads to incorrect splicing

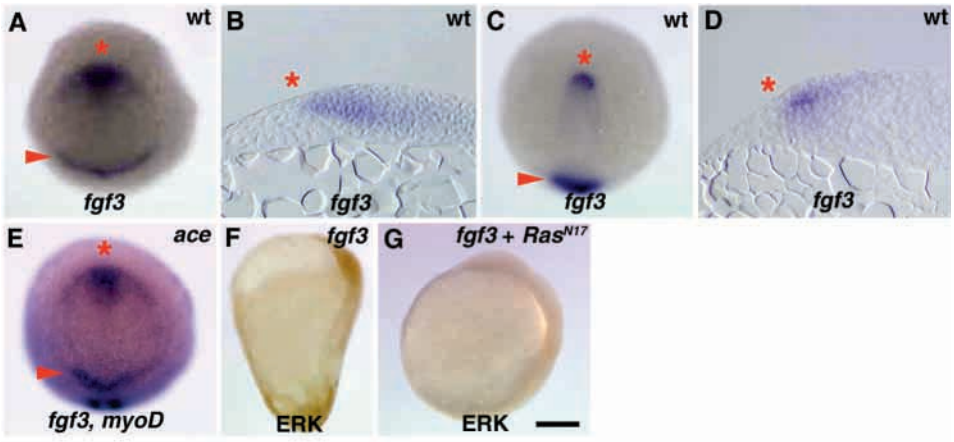

Fig. 4. Expression pattern and the activity of zebrafish *fgf3*. (A-E) Expression pattern of *fgf3*. (A,C,E) Dorsal view of the head region. (A,B,E) Tailbud stage and (C,D) five-somite stage, wild-type embryos (A-D) and *ace* mutant embryo (E). *ace* homozygous mutants were recognised by fragmented *myoD* staining in adaxial cells. (B,D) Sagittal sections taken from the embryo shown in A,C, respectively. *fgf3* expression in the ANB is maintained normally in *ace* mutant embryo. (F,G) Lateral view, dorsal towards the right; ERK is activated in the whole embryo when injected *fgf3* (F); the effect is cancelled by co-injection of Ras^{N17} RNAs (G). As shown in F, Fgf3 exhibits strong posteriorizing and dorsalizing effects when overexpressed at early stages (S. K. et al., unpublished). Asterisks indicate positive staining in the ANB and arrowheads indicate that in the MHB. Scale bar: 100 μm in A,C,E-G; 30 μm in B,D.

generating a truncated non-functional protein (Reifers et al., 1998). Because, at the five-somite stage, homozygous *ace* mutants can not be distinguished morphologically from wild-type embryos, we examined the expression pattern of *myoD* in the trunk region. It has been reported that the adaxial cells of homozygous *ace* mutants show reduced and fragmented expression of *myoD* (Reifers et al., 1998). Although the intensity of ERK staining varies to some degree and tends to be weaker as compared with wild-type siblings, a substantial amount of positive reactions are reproducibly observed in the ANB (7/10, Fig. 3A,B) of *ace* mutants. Western blot analysis revealed that the level of ERK activation was about half of the wild type in *ace* mutants. These results indicated that Fgf signalling remains activated in the ANB in the absence of Ace/Fgf8.

Zebrafish *fgf3* is expressed in the wild-type and *ace* ANB

The temporal and spatial pattern of ERK activation correlated well with that of *fgf3* expression in the ANB (compare Fig. 1C, D with Fig. 4C,D) (Shanmugalingam et al., 2000). Zebrafish *fgf3* starts to be expressed at the end of the gastrulation in the anterior head region, the anterior forebrain and MHB (Fig. 4A), and its expression persists until around the 10-somite stage (Fig. 4C). Histological sections reveal that the anterior staining is located in the ANB (Fig. 4B,D), where *fgf8* is also expressed (Shanmugalingam et al., 2000). Importantly, *fgf3* expression is maintained in the ANB of *ace* homozygous embryos at the tailbud stage (10/10, Fig. 1E) and mid-somite stage (10/10), suggesting that Fgf3 may compensate for the function of Fgf8 in the *ace* ANB. Indeed, Fgf3 is a potent activator of ERK: *fgf3* RNA injection into one- to two-cell stage embryos induced ERK activation in entire embryo (25/25, Fig. 4F), while this activation was abolished by co-injection of Ras^{N17} RNAs (38/38, Fig. 4G).

Inhibition of Ras-dependent pathway suppresses the development of subpallial telencephalon

To explore the roles of Fgf signalling in zebrafish forebrain development, we examined the effects of Ras^{N17} injection. Morphologically, Ras^{N17}-injected embryos showed obvious defects in the MHB and tail region. In most cases, the tail and yolk tubes did not extend well and the segmented structures in the trunk was hardly observed, indicating that the disruption of Fgf signalling cascade affected mesodermal tissues. Furthermore, we observed that the forebrain and midbrain region tended to be enlarged, probably owing to reduced posteriorising signals derived from the non-axial mesoderm (Woo and Fraser, 1997; Koshida et al., 1998). In addition to the MHB and tail, in more than half of Ras^{N17}-injected embryos the telencephalic region became turbid at 33 hpf, especially in the ventral part of the telencephalon (Fig. 5A,B). DNA fragmentation analysis revealed that apoptotic cells were induced by overexpression of Ras^{N17} (8/11, Fig. 5C,D). Apoptotic cells were frequently observed in the ventral part of telencephalon but less in the dorsal. However, at 26 hpf, there was little apoptotic cell detected in the entire telencephalon of Ras^{N17}-injected embryos (18/18, Fig. 5E,F).

To determine whether the telencephalic patterning was altered before the appearance of apoptosis, we stained injected embryos with forebrain markers at different developmental stages between bud to 26 hpf. In situ hybridisation analyses with 1-day-old embryos revealed that, in Ras^{N17}-injected embryos, development of the subpallial telencephalon was severely affected. In zebrafish, the *distal-less* related gene, *dlx2*, is normally expressed in the subpallial telencephalon and diencephalon (Akimenko et al., 1994). Overexpression of Ras^{N17} reduced or abolished *dlx2* expression in the telencephalon (42/60, Fig. 5G,H), while the expression in the diencephalon was unaffected. Overexpression of Ras^{N17} also reduced the expression of zebrafish *nk2.1b* (Rohr et al., 2001), which is a basal telencephalic marker related to mouse *Nkx2.1* (Shimamura et al., 1995; Rubenstein et al., 1998) (61/64; Fig. 5I,J). Contrary to the subpallial markers, the expression domains of *emx1* (Morita et al., 1995), *eomesodermin* (*eom*) and *T-brain-1* (*tbr1*) (Mione et al., 2001), which are normally confined to the pallial region of the telencephalon at 26 hpf, nearly covered the entire region of the telencephalon in Ras^{N17}-injected embryos (32/37 for *emx1*, Fig. 5K,L; 25/25 for *eom*, Fig. 5M,N; 24/24 for *tbr1*, Fig. 5O,P).

The loss of the subpallial telencephalon was detected as

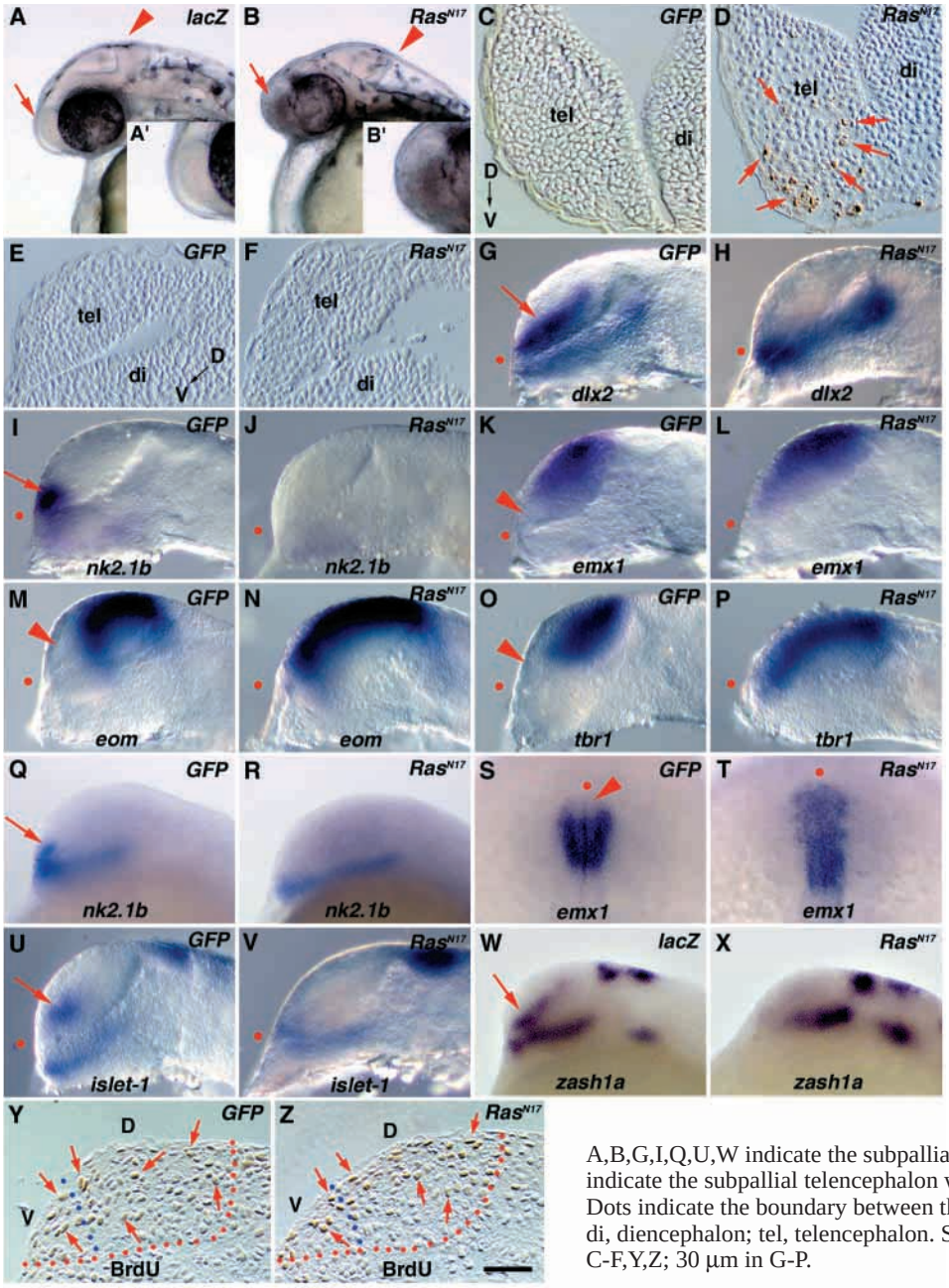

Fig. 5. Patterning and neurogenesis in the telencephalon in *Ras*^{N17}-injected embryos. Injected RNA is shown in the upper right and the probe used is indicated at the bottom. (A,B) Lateral view of the head region; *Ras*^{N17}-injected embryo exhibits the turbid telencephalon, truncation of a part of the eye and no MHB (arrowheads in A,B) in the head region. A′ and B′ are high magnification views of the telencephalic region of A,B respectively. (C-F) Sagittal section of the embryos detected for DNA fragmentation at 33 hpf (C,D) and 26 hpf (E,F); apoptotic cells are detected in the telencephalon of the *Ras*^{N17}-injected embryo at 33 hpf (arrows in D) but not at 26 hpf (F). (G-X) Lateral views (G-R,U-X) and dorsal views (S,T) of the head region; whole-mount in situ hybridisation was performed at the 26 hpf (G-P,U,V), 14-somite (Q,R), 15-somite (S,T) and 12-somite (W,X) stages. Subpallial telencephalic expressions of *dlx2* (G,H), *nk2.1b* (I,J,Q,R), *islet-1* (U,V) and *zash1a* (W,X) are lost in the *Ras*^{N17}-injected embryo while the pallial telencephalic markers, *emx1* (G,H,S,T), *eom* (M,N) and *tbr1* (O,P) cover the entire telencephalon. (Y,Z) Sagittal sections of the telencephalon showing BrdU labelling at the seven- to eight-somite stage after injection of *GFP* (Y) and *Ras*^{N17}RNAs (Z). The labelled cells are indicated by arrows. The telencephalic region is marked by broken red lines. The ventral (V) and dorsal (D) regions we defined in the sections are separated by broken blue lines. The 'ventral' corresponds approximately to the region showing strong ERK staining. Arrows in A,B,G,I,Q,U,W indicate the subpallial telencephalon, arrowhead in K,M,O,S indicate the subpallial telencephalon which is negative for *emx1*, *eom* or *tbr1*. Dots indicate the boundary between the telencephalon and ventral diencephalon. di, diencephalon; tel, telencephalon. Scale bar: 50 μm in A,B,Q,R,W,X; 10 μm in C-F,Y,Z; 30 μm in G-P.

early as segmentation stages. In normal embryos, *nk2.1b* expression in the telencephalon starts to be detected around the 14-somite stage (Rohr et al., 2001). However, *nk2.1b* expression was not detected throughout development in *Ras*^{N17}-injected embryos (20/20; Fig. 5Q,R). Consistently, *dlx2* expression in the telencephalon, which starts to be activated at around the 15-somite stage (Akimenko et al., 1994), was not observed in *Ras*^{N17}-injected embryos at any stages (30/36, data not shown). In normal embryos, *emx1* is first expressed in the telencephalic region, and, by the 10-somite stage, the expression is downregulated in the anteriormost of the forebrain, which may be fated to the subpallial telencephalon (Morita et al., 1995; Shanmugalingam et al., 2000). This downregulation, however, was never observed in *Ras*^{N17}-injected embryos (29/29; Fig. 5T). Thus, the regionalisation within the telencephalon was stopped at its early phase (at least as early as 10-somite stage of development) when Ras/MAPK cascade was blocked. During these early stages, inhibition of Ras pathway may affect cell growth in the telencephalic region.

Table 1. Cell proliferation in the telencephalon of *Ras*^{N17}-injected embryos

	Ventral	Dorsal
GFP injected	32.5%±3.9	29.5%±4.7
Ras^{N17} injected	33.4%±6.7	34.2%±4.9

Mitotic cells were counted 3 hours after injection of BrdU at the tailbud stage. Six embryos for *GFP* and seven embryos for *Ras*^{N17} were examined and the proportion of BrdU-positive cells were averaged in the ventral and dorsal part of the telencephalon.

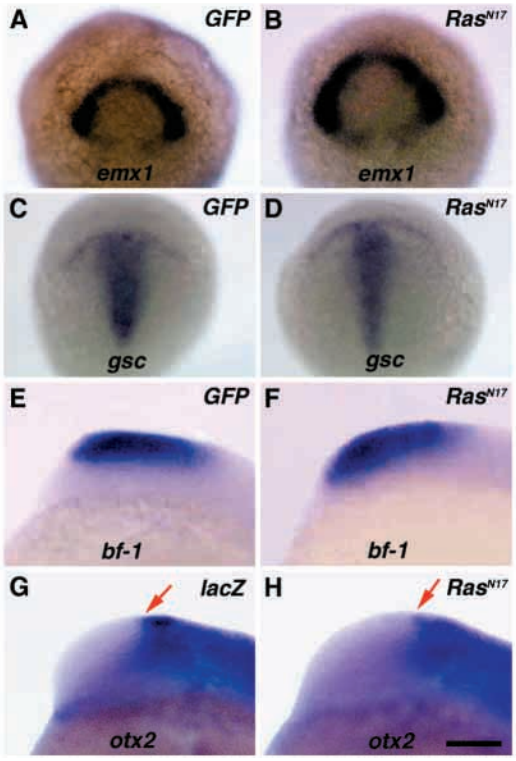

Fig. 6. Telencephalic territory is normally specified in *Ras*^{N17}-injected embryo. Injected RNA is shown in the upper right and the probe used is indicated at the bottom. (A-D) Dorsal views of the head region at tailbud stage: *emx1* expression in the prospective telencephalon is not altered by *Ras*^{N17} injection (A,B); *gsc* expression in the prechordal plate is not altered by *Ras*^{N17} injection (C,D). (E,F) Lateral views of the head region at the five-somite stage, anterior towards the left; *bf-1* expression in the telencephalon is normally seen in *Ras*^{N17}-injected embryo. (G,H) Lateral views of the head region at 15-somite stage, anterior towards the left; *otx2* expression in the anterior forebrain is normally downregulated in *Ras*^{N17}-injected embryos. Arrows indicate the mid-diencephalon. Scale bar: 75 μm in A-D; 50 μm in E-H.

To test this, we injected BrdU into *Ras*^{N17}-injected embryos at tailbud stage and examined the proportion of labelled cells after 3 hours' incubation (8-10 somite stage). However, we did not find any significant difference in cell proliferation in the telencephalon, either in ventral or dorsal region (Fig. 5Y,Z; Table 1).

In addition to the region-specific markers, Ras^{N17} affected markers for neuronal differentiation in the telencephalon. *islet-1* expression around the anterior commissure (Inoue et al., 1994) (Fig. 5U) was not observed in *Ras*^{N17}-injected embryos at 26 hpf (19/20; Fig. 5V). *zash1a* expression in the telencephalon was also undetectable in *Ras*^{N17} injection (20/24; Fig. 5W,X). *zash1a*, one of the zebrafish genes related to *Drosophila achaete-scute* (Campuzano and Modolell, 1992), starts to be activated in the part of the subpallial telencephalon at 12-somite stage (Allende and Weinberg, 1994). These data demonstrated that Ras^{N17} suppressed the differentiation of putative subpallial neurones.

Inhibition of Ras-dependent pathway does not affect the formation of telencephalic territory

In contrast to the regionalisation within the telencephalon, early overall patterning of the forebrain appeared normal in *Ras*^{N17}-injected embryos. As described above, *emx1*, an early

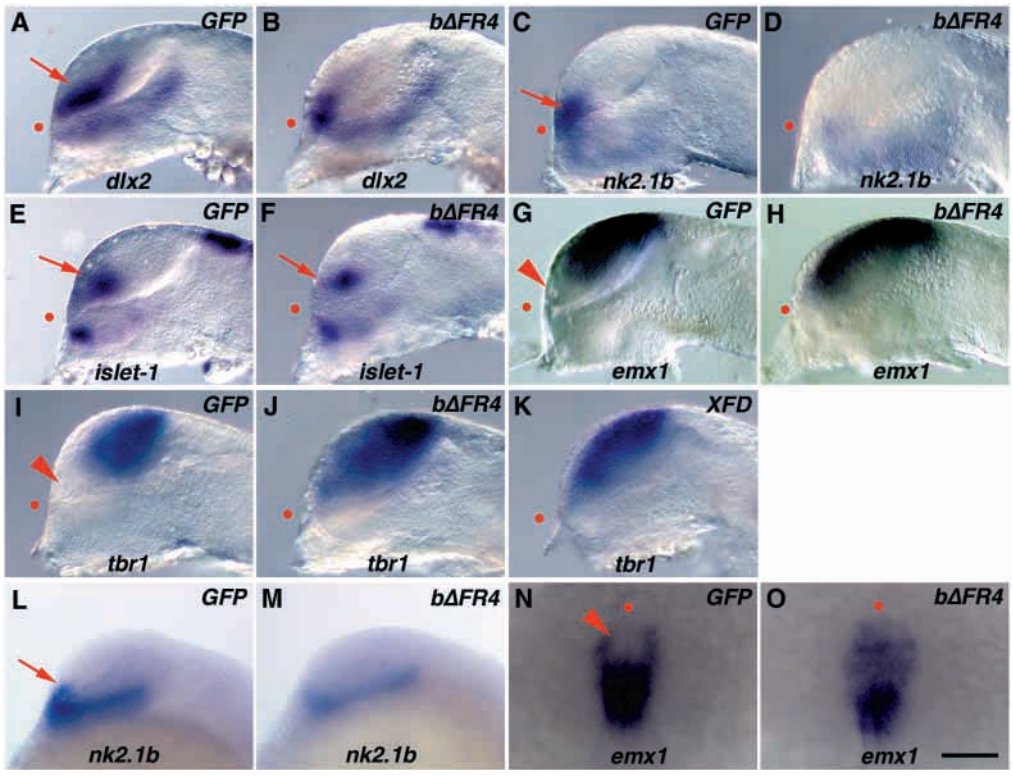

Fig. 7. Patterning and neurogenesis in the telencephalon in the *b*Δ*FR4*- and *XFD*-injected embryos. Injected RNA is shown in the upper right and the probe used is indicated at the bottom. Lateral view (A-M) and dorsal view (N,O) of the head region are shown. Whole-mount in situ hybridisation was performed at the 26 hpf (A-K), 14-somite (L,M) and 15-somite (N,O) stages. Subpallial telencephalic expressions of *dlx2* (A,B), *nk2.1b* (C,D,L,M) and *islet-1* (E,F) are suppressed in the *b*Δ*FR4*-injected embryo, while the pallial telencephalic markers, *emx1* (G,H,N,O), and *tbr1* (I,J) cover the entire telencephalon. Similarly, in the *XFD*-injected embryo, *tbr1* expression is expanded (K). Arrows indicate the subpallial telencephalon, and arrowheads indicate the subpallial telencephalon, which is negative for *emx1*, *eom* or *tbr1*. Dots indicate the boundary between the telencephalon and ventral diencephalon. Scale bar: 30 μm in A-K,N; 50 μm in L,M.

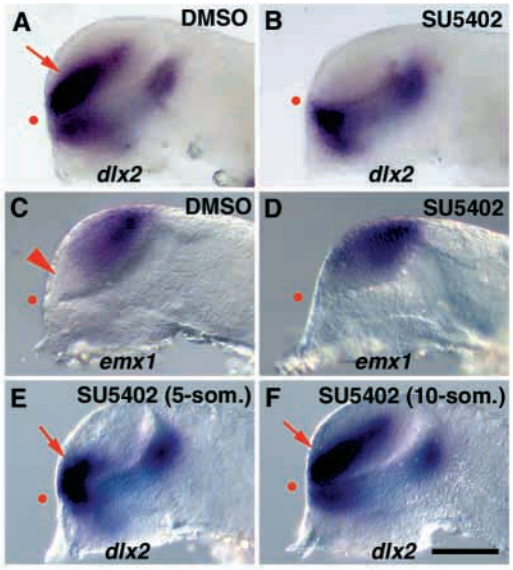

Fig. 8. Patterning and neurogenesis in the telencephalon after treatment of SU5402. The probe used is indicated at the bottom. All embryos are lateral views of the head region at 26 hpf. Embryos were injected with SU5402 (B,D) or DMSO (A,C) in the head region at tailbud stage (A-D). In E,F, the embryos were soaked in medium containing SU5402 at the five- and 10-somite stages, respectively. (A-D) *dlx2* expression in the subpallial telencephalon is abolished by SU5402, while *emx1* reaches the edge of the telencephalon after SU5402 treatment. Note the smaller telencephalon is frequently seen in treated embryos (B,D). (E,F) *dlx2* expression is greatly reduced when the embryos are treated with SU5402 at the five-somite stage (E), while the expression is relatively normal when treated at the 10-somite stage (F). Arrows indicate the gene expression in the subpallial telencephalon. Dots indicate the boundary between the telencephalon and ventral diencephalon, while arrowheads indicate the ventral region that is negative for *emx1*. Scale bar: 50 μm.

telencephalic marker, was normally activated at the tailbud stage in the prospective telencephalic region of the *Ras^{N17}*-injected embryos (21/22; Fig. 6A,B). At this stage, we observed normal expression of *gsc* (Stachel et al, 1993) (21/21; Fig. 6C,D), *dkk-1* (Shinya et al., 2000) (28/28) and *hlx1* (Fjose et al., 1994) (20/20) in injected embryos, indicating that Ras^{N17} did not affect the development of the underlying prechordal plate that is known to be important in establishment of the telencephalic region (Shinya et al., 2000). The expression of another early telencephalic marker, *bf-1*, which is expressed in the telencephalon and a part of eyes (Toresson et al., 1998), was not altered by *Ras^{N17}* injection when examined at the five-somite stage (20/20; Fig. 6E,F) and 24 hpf (41/41, data not shown). Furthermore, downregulation of *otx2* at the mid-somite stage in the region fated to the telencephalon and ventral diencephalon (Mori et al., 1994) normally occurred in injected embryos (33/34; Fig. 6G,H). Thus, the establishment of telencephalic and diencephalic territories normally takes place even when the Ras/MAPK cascade is suppressed.

We also confirmed that Ras^{N17} did not affect the development of other parts of CNS: for example, the expression of sonic hedgehog (*shh*) in the ventral spinal cord and ventral diencephalon (Krauss et al., 1993) was normal in *Ras^{N17}*-injected embryos (18/18, data not shown).

bΔFR4, XFD and SU5402 produced the same phenotypes as those with Ras^{N17}

When specific inhibitors to Fgfr-mediated signal were employed, essentially the same results were obtained (Table 2). In *bΔFR4*-injected embryos, expression of *dlx2* (Fig. 7A,B), *nk2.1b* (Fig. 7C,D) and *islet-1* (20/30, Fig. 7E,F) in the subpallial telencephalon at 26 hpf was suppressed while pallial markers, *emx1* (Fig. 7G,H), *eom* (23/29) and *tbr1* (Fig. 7I,J) expression covered the entire telencephalon. These effects were already observed at mid-somite stage. In the *bΔFR4*-injected embryos, *nk2.1b* expression was suppressed (15/18, Fig. 7L,M) at the 14-somite stage and *emx1* was expressed throughout the telencephalon at the 15-somite stage (43/44, Fig. 7N,O). By contrast, the territory of the telencephalon was established normally, judging from the expression pattern of *emx1* at tailbud stage, *bf-1* at the five-somite stages and *otx2* at the 15-somite stage (data not shown). The same phenotypes were obtained when *XFD* RNAs were injected (Table 2; Fig. 7K) (7/13 for *tbr1*).

Although the size of telencephalon tended to be smaller as compared with overexpression of Ras^{N17} and bΔFR4, the injection of SU5402 (10 mg/ml) into the anterior head region at the tailbud stage (see Fig. 2D) gave rise to similar phenotypes in gene expressions of *dlx2* (20/26; Fig. 8A,B), *emx1* (9/13; Fig. 8C, D) and *islet-1* (11/18, data not shown).

bΔFR4 and SU5402 also induced apoptosis in the ventral part of telencephalon, but the effect was weaker when compared with that in *Ras^{N17}*-injected embryos.

Among the RNAs injected, *XFD* seems to be less effective

Table 2. The effects of RNA injection on telencephalic gene expressions

	RNA injected					
	Ras^{N17}		*bΔFR4*		*XFD*	
Subpallial markers	*dlx2*	*nk2.1b*	*dlx2*	*nk2.1b*	*dlx2*	*nk2.1b*
Normal expression	30.0%	4.7%	13.3%	9.4%	72.2%	0
Reduced expression	31.7%	12.5%	76.7%	37.5%	27.8%	69.2%
No expression	38.3%	82.8%	10.0%	53.1%	0	30.8%
*n**	60	64	30	32	18	13
Pallial markers	*emx1*	*tbr1*	*emx1*	*tbr1*	*emx1*	*tbr1*
Normal expression	13.5%	0	11.1%	8.0%	53.3%	46.2%
Expanded expression	86.5%	100.0%	88.9%	92.0%	46.7%	53.8%
*n**	37	24	45	25	15	13

*Total number of injected embryos.

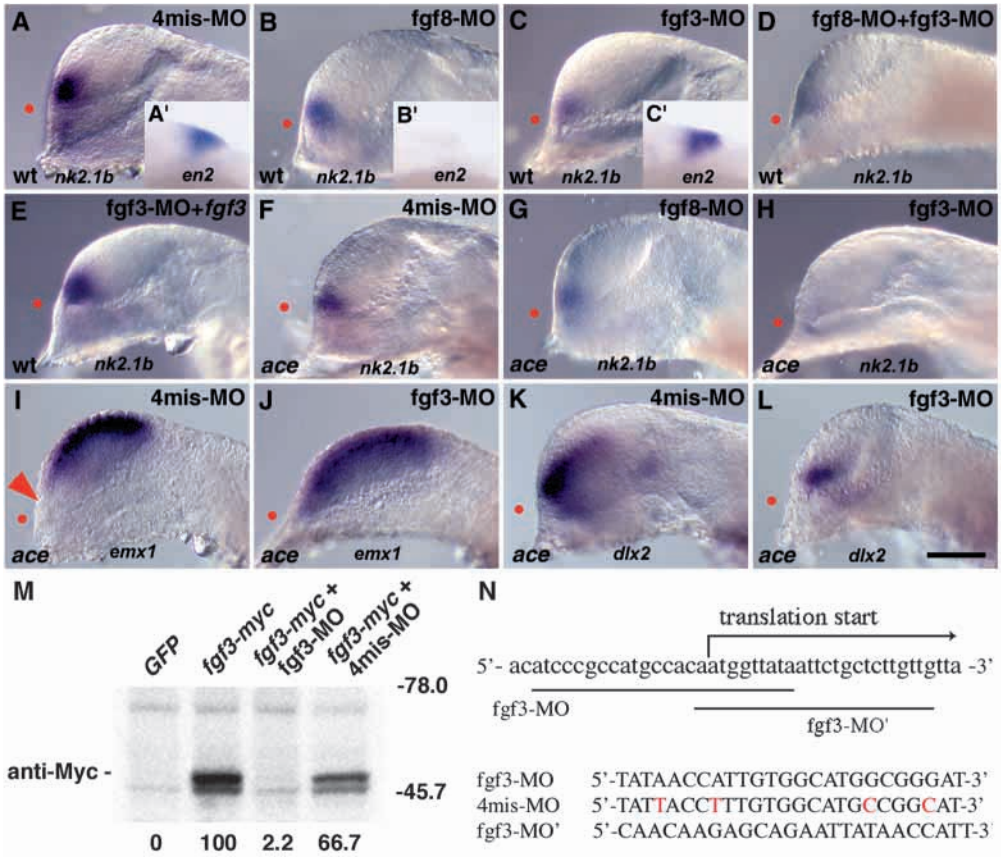

Fig. 9. Gene expression in the embryos injected with morpholino-modified (MO) antisense oligonucleotides. Injected MO is shown in the upper right and the probe used is indicated at the bottom. Lateral views of the head region at 26 hpf. Embryos were injected with 4mis-MO (A,F,I,K), fgf8-MO (B,G), fgf3-MO (C,H,J,L), fgf8-MO and fgf3-MO (D), and fgf3-MO and *fgf3* mRNA (E). (A-E) Wild-type embryos were used. Injection of either fgf8-MO (B) or fgf3-MO (C) reduces *nk2.1b* expression. However, reduction of *nk2.1b* is further enhanced when both fgf8-MO and fgf3-MO was co-injected (D). (A′-C′) *en2* expression after 4mis-MO (A′), fgf8-MO (B′) and fgf3-MO (C′) injection. *en2* expression is reduced in fgf8-MO-injected embryo but remains unchanged in fg3-MO-injected embryo. (E) *nk2.1b* expression is rescued by co-injection of fgf3-MO and *fgf3* RNAs. (F-H) Embryos from *ace* heterozygous parents were used; fgf3-MO but not fgf8-MO injection enhances the reduction of *nk2.1b* in some embryos (17/58). (I-L) Injected embryos from *ace* heterozygous parents were double-stained with *en2* and *emx1* (I,J) or *dlx2* (K,L), and homozygous mutants were identified by a lack of *en2* expression in the MHB. An arrowhead in I indicates the subpallial telencephalon, which is negative for *emx1*. Dots indicate the boundary between the telencephalon and ventral diencephalon. Scale bar: 50 μm. (M) Western blot analyses of translation of injected *fgf3-myc*. RNA injections were carried out at the one-cell stage. The homogenates were prepared from injected blastula. Anti-Myc antibody detects a major band about 50 kDa which is not present in control injection (*GFP* RNAs). Relative intensity of the major band is shown at the bottom of each lane. Relative intensity was normalised by a nonspecific minor band that appears in all lanes and insensitive to morpholino injection. (N) Morpholino oligonucleotides used in the present study. Red letters in 4mis-MO indicate mismatch nucleotides to fgf3-MO.

(Table 2). Especially, in the case of *dlx2*, only five out of 18 embryos injected with *XFD* RNAs showed reduced expression (Table 2). This could reflect the fact that the inhibitory effect of XFD on ERK activation does not last long (Fig. 2I). In spite of these, all inhibitors showed the similar tendency and, thus, we conclude that Fgf signalling through Ras/MAPK cascade is required for the development of the subpallial telencephalon.

The subpallial telencephalon requires Fgf signalling at early segmentation stages

Anti-dpERK staining revealed that ERK activation reached a level peak at the five-somite stage and, thereafter, gradually decreased. To address when Fgf signalling might be required for development of the subpallial telencephalon, we treated embryos with SU5402 at tailbud, five-somite, 10-somite and 15-somite stages, and its effect on *dlx2* expression was examined. In this series of experiments, we soaked embryos in 0.1 mg/ml or 0.2 mg/ml SU5402 in 1/3 Ringer's solution for 10 minutes. This worked well, and the resulting phenotype in the telencephalon was identical to that obtained with injection of SU5402.

As summarised in Table 3, early treatment (bud to 5-somite) with SU5402 led to loss or severe reduction of *dlx2* in the subpallial telencephalon (Fig. 8E). By contrast, treatment from 10- and 15-somite stage gave rise to normal *dlx2* expression in this region (Fig. 8F). Thus, Fgf signalling up to the five-somite stage is crucial for the establishment of the subpallial telencephalon but, thereafter, *dlx2* expression can be maintained without Fgf signalling.

Functions of Fgf3 and Fgf8 in the development of subpallial telencephalon and MHB

As described above, *fgf8* and *fgf3* are co-expressed in zebrafish ANB, and ERK activation is maintained in *ace* mutants. This led us to analyse the role of Fgf3 in the development of the subpallial telencephalon. To do this, we blocked the function of Fgf3 by using antisense morpholino-modified oligonucleotides (morpholino) that were targeted to the zebrafish *fgf3* gene (fgf3-MO; Fig. 9N). Morpholinos have been reported to work well as effective and specific translational inhibitors in zebrafish (Nasevicius and Ekker, 2000; Sakaguchi et al., 2001). Indeed, injection of *fgf8*-targeted morpholino (fgf8-MO) at a concentration of 20 μg/μl (about 10 ng injected) resulted in a phenocopy of *ace* mutants, in which *nk2.1b* expression in the subpallial telencephalon was reduced (29/29; Fig. 9B), although the phenotype tended to be

Table 3. Alteration of dlx2 expression in the telencephalon of SU5402-soaked embryos

Treated stages	I	II	III	n
Tailbud	46.7%	53.3%	0%	15
Five somites	20.0%	45.0%	35.0%	20
10 somites	0%	0%	100.0%	21
15 somites	0%	0%	100.0%	21

Embryos at each developmental stage were treated with 0.1 or 0.2 mg/ml SU5402 for 10 minutes and dlx2 expression was analysed in the telencephalon at 24 hours post fertilisation.

I, no *dlx2* expression; II, reduced *dlx2* expression; III, normal *dlx2* expression.

n indicates the total number of the treated embryos.

milder (compare Fig. 9B with 9F). Injection of 10 μg/μl fgf3-MO (about 5 ng injected) also reduced the *nk2.1b* expression (28/29; Fig. 9C). However, co-injection of fgf8-MO and fgf3-MO resulted in more severe reduction in *nk2.1b* expression (29/29; Fig. 9D). These results indicate a co-operative action of Fgf3 and Fgf8 on *nk2.1b* expression.

In the MHB, the effects of fgf8-MO and fgf3-MO were different from each other. Injection of fgf8-MO reduced the expression of *en2* (11/11; Fig. 9B′) (Ekker et al., 1992) phenocopying the *ace* mutant, while that of fgf3-MO did not affect the expression (23/23; Fig. 9C′).

To test the specificity of the phenotype, we made another fgf3-MO designed against more 3′ sequence (fgf3-MO'; Fig. 9N). fgf3-MO' exhibits similar effects on *nk2.1b* expression in wild-type (32/41) and fgf8-MO-injected (22/26) embryos. We then constructed a cDNA encoding Fgf3 tagged with Myc epitope at the C terminus, because an antibody against zebrafish Fgf3 is not available. Western blot analyses were performed with the embryos injected with either *fgf3-myc* RNAs alone or *fgf3-myc* and fgf3-MO. Co-injection of fgf3-MO completely blocked the translation of injected *fgf3-myc* RNAs, while the degree of inhibition much decreased in the case of 4mis-MO in which a four-base mismatch was introduced into fgf3-MO (Fig. 9M). We also confirmed that 4mis-MO, when injected, did not affect *nk2.1b* expression (Fig. 9A). Furthermore, the effect of fgf3-MO was diminished when *fgf3* RNAs (5 ng/μl, about 2.5 pg per embryo) were co-injected (9/18, Fig. 9E). We were unable to obtained 100% rescue because the increased amount of *fgf3* RNAs suppressed the head development in injected embryos even in the presence of fgf3-MO, probably owing to strong posteriorising and dorsalizing effects of Fgf3 at the gastrulation stage (S. K., M. S., M. Nikaido, N. Ueno, S. Schulte-Merker, A. K. and H. T., unpublished). Finally, we injected fgf3-MO (10 μg/μl) in embryos obtained from *ace* heterozygous crosses. Seventeen out of 58 injected embryos showed no or faint *nk2.1b* expression (Fig. 9H), while such enhanced phenotype was not observed by injection of fgf8-MO (54/54; Fig. 9G).

Finally, we examined *emx1* and *dlx2* expression in fgf3-MO-injected *ace* homozygous embryos. The expression of these two markers are relatively normal in *ace* mutants at 26 hpf. The *ace* homozygous embryos were identified by a lack of *en2* expression in the MHB in double-stained embryos, as fgf3-MO alone does not affect *en2* expression (Fig. 9C). Like SU5402 treatment, injection of fgf3-MO resulted in ventral expansion of *emx2* (9/9; Fig. 9J) and reduction of *dlx2* (11/18 for severe and 7/18 for mild reduction, Fig. 9L) expression in *ace* mutants, while no such effect was observed in control injections (18/18 for *emx1* and 11/13 for *dlx2*; Fig. 9I,K). Thus, the expression of *exm1* and *dlx2* is more dependent on Fgf3.

DISCUSSION

In the present study, we report for the first time the spatial pattern of ERK activation in fish development. Strong ERK activation is detected in the mesoderm, ANB, MHB and tailbud in developing zebrafish embryos. Like *Xenopus* embryos (Christen and Slack, 1999), ERK activation at zebrafish segmentation stages depends on Fgf signalling. We then examine the role of Fgf signalling in forebrain development by use of inhibitors to Fgf signalling. Shanmugalingam et al. (Shanmugalingam et al., 2000) have shown that, in *ace* embryos, differentiation of the basal telencephalon and some putative telencephalic neurones were disrupted. In our study, the phenotype obtained by suppression of Fgf signalling encompasses that reported in *ace* mutants. In addition, we observe overall loss of subpallial fate and increased apoptosis in the ventral telencephalon, which are not seen in *ace* embryos. These data demonstrate that Fgf signalling in the ANB is required for the development of the subpallial telencephalon.

Fgf8 is not a sole Fgf involved in ERK activation in the ANB

As in other vertebrates, zebrafish *fgf8* is expressed during gastrulation in the mesoderm, presumptive MHB and telencephalon. (Fürthauer et al., 1997; Reifers et al., 1998). Expression in the CNS is prominent in the MHB and in the anteroventral telencephalon at segmentation stages (Reifers et al., 1998; Shanmugalingam et al., 2000). ERK activation appears to follow the expression pattern of *fgf8* up to mid-somite stage, suggesting that *fgf8* is responsible for ERK activation. However, the analysis with *ace* mutants, in which no functional Fgf8 is produced (Reifers et al., 1998), suggests that Fgf8 is not a sole Fgf responsible for ERK activation. Although the level of activation tends to be weaker, a substantial amount of ERK activation persists in the ANB of *ace* homozygous mutant. Expression analysis and overexpression experiments suggest that Fgf3 is one of the candidates involved in ERK activation in the ANB.

After mid-somite stage, the level of ERK activation gradually decreases in the MHB and then in the ANB, whereas *fgf8* expression remains high in these regions. This suggests that Fgfs, albeit expressed, do not necessarily activate their signalling pathway. Alternatively, ERK activation may not represent all Fgf activity, or antibody labelling may not detect low levels of ERK activation. In fact, Fgfs are known to use various signalling cascades other than Ras/MAPK such as phosphatidylinositol 3′ kinase (Klint and Claesson-Welsh, 1999).

Roles of Fgf signalling in normal development of the subpallial telencephalon

Analysis with telencephalic markers reveals loss of the subpallial fate after treatment with inhibitors to Fgf receptors. In addition to region specific markers, disruption of Fgf signalling reduces or abolishes the expression of differentiation

markers specific to putative subpallial neurones. The effects seem direct because the underlying prechordal plate develops normally in treated embryos as judged by gene expression. The present results, therefore, indicate that Fgf signalling in the ANB is required for differentiation of subpallial neurones as well as establishment of the subpallial region.

There are at least three possible explanations for the phenotype in affected embryos: (1) the ventral telencephalon fails to acquire subpallial fate and develops into the pallium; (2) the subpallial region is established but disappears due to cell death; and (3) cells in the subpallium fail to proliferate and remains in a small number, while development of the pallial telencephalon proceeds normally. As cell death in the telencephalon is detected only after loss or reduction of the subpallial markers, the second possibility seems less likely. The detailed analysis of cell proliferation and movements during normal development of the subpallial telencephalon has not been done in fish. Thus, we cannot rule out either the first or third explanations. However, the following two observations favour the first possibility. First, inhibition of Ras pathway does not affect cell proliferation in the telencephalon at early segmentation stages (Table 1). Second, in affected embryos, subpallial markers such as *dlx2* and *nk2.1b* are never detected at any stages examined, suggesting that the subpallial fate is not induced from the beginning.

In the present study, inhibition of the Fgf signalling affects only a part of the telencephalon, the subpallial region. Cells in the subpallium are shown to derive from the ANB. The row 1 cells in the ANB contributes to the anteriormost subpallial telencephalon (Houart et al., 1998). The precise lineage analysis by Whitlock and Westerfield (Whitlock and Westerfield, 2000) has revealed that cells in the ventral telencephalon come from the anterior margin of the neural plate at the five-somite stage, whereas more posterior margin is fated to the dorsal telencephalon. Their fate map of the ventral telencephalon well fits with ERK activation domain that is narrower than *emx1*-positive domain (a maker for the entire telencephalon at early stages). Thus, it is reasonable to say that the effect of Fgf inhibition was observed in the region where Ras/MAPK pathway is activated.

Brief treatment of developing embryos with SU5402 reveals that Fgf signalling is not required for subpallial development after 10-somite stage. The crucial period coincides with the stage when the strongest activation of ERK is observed. However, it has been reported that the same treatment at 18-somite stage still causes some defects in axon guidance between anterior commissure and post-optic commissure (Shanmugalingam et al., 2000). Thus, it is likely that a crucial period for requirement of Fgf signalling varies, depending on the region and developmental processes of the telencephalon.

Fgf signalling may not be required for induction of the telencephalic territory in zebrafish

Studies in mice have provided evidence that the anterior neural ridge (ANR), which is located in the anterior boundary between the neural and non-neural ectoderm, plays an important role in induction of the telencephalon. Shimamura and Rubenstein (Shimamura and Rubenstein, 1997) demonstrated by in vitro culture method that the ANR in mice is necessary and sufficient for the induction of telencephalic *bf-1* expression. In zebrafish, the most anterior neural cells in the ANB, called row 1 cells, were found to possess the similar inducing ability to the mouse ANR (Houart et al., 1998). The ablation of row 1 cells resulted in the loss of telencephalic markers and apoptosis in the anterior head region (Houart et al., 1998). As in vitro experiments in mice have demonstrated that Fgf8-soaked beads mimic nearly all activity of the ANR in mammals (Shimamura and Rubenstein, 1997), Fgf signalling has been proposed to account for the inducing ability of the ANR.

However, we observe in the present study that the establishment of the telencephalic and diencephalic territories normally proceeded in the Ras^{N17}-injected embryos, as indicated by normal expression patterns of *bf1*, *emx1* and *otx2* at early segmentation stages. This suggests more restricted functions of Fgf signalling in telencephalic development. Indeed, no expression of any *fgf* or activation of ERK is detected in the ANB at the gastrula stage when the overall patterning of the CNS is specified. Consistent with this, SU5402 treatment at mid-gastrula (75%-epiboly) stage did not affect *emx1* expression at tailbud stage (data not shown). Therefore, although involvement of low level of Fgf signal can not be ruled out, our findings suggest that, in zebrafish, Fgf signalling is mainly required for regionalisation but not for induction of the telencephalon.

Overlapping and distinct functions of Fgfs expressed in the CNS

Our antisense experiments suggest that Fgf3 co-operates with Fgf8 in the ANB. The antisense experiments seemed to work well in the present study. We are able to generate a phenocopy of *ace* mutant by injecting fgf8-MO, and fgf3-MO is able to inhibit translation of injected *fgf3* RNAs in a sequence-specific manner. Furthermore, we recently demonstrated that *casanova* (226D7)-MO injection phenocopied *casanova* mutant, a complete loss of endodermal precursors (Sakaguchi et al., 2001).

Although the injection of fgf8-MO or fgf3-MO alone results in slight reduction of *nk2.1b* expression, severe reduction of *nk2.1b* is observed after co-injection of fgf8-MO and fgf3-MO. The results demonstrate that both Fgf8 and Fgf3 are required for normal *nk2.1b* expression of the subpallial telencephalon. It has also been revealed that *emx1* and *dlx2* expressions are more dependent on Fgf3. These data may account for relatively mild defects in the subpallial telencephalon of *ace* mutants. In the MHB, however, zebrafish Fgf8 has a major role as indicated by the phenotype of *ace* mutant, even though *fgf3* expression is detected in the region (Fig. 4A,C). In support of this, the expression of *en2* persists in fgf3-MO-injected embryos while the expression is reduced in fgf8-MO-injected embryos. Thus, Fgf8 and Fgf3 possess overlapping and distinct functions in the ANB and MHB, respectively. Considering that there are certainly further Fgfs in zebrafish that have yet to be identified, further molecular and genetic analyses will be required to elucidate full functions of Fgf signalling in the developing CNS.

We thank Drs S. Wilson and C. Houart for useful discussions and critical reading of the manuscript, and Dr K. Rohr for providing an unpublished probe for zebrafish *nk2.1b*. We are also grateful to Drs M. Mishina, H. Mori, H. Okamoto, S. Krauss, M. Hibi and M. Mione for providing probes, Dr E. Amaya for *XFD* cDNA, Dr H. Okamoto

for *bΔFR4* cDNA, Drs T. Deng and M. Karin for *Ras^{N17}* cDNA, and Dr M. Kobayashi for providing *ace* mutants. This work was supported in part by Pioneering Research Project in Biotechnology from the Ministry of Agriculture, Forestry and Fisheries of Japan, and by grants-in-aids from the Ministry of Education, Science, and Culture of Japan. M. S. is supported by the Research Fellowships of the Japan Society for the Promotion of Science for Young Scientists.

REFERENCES

Akimenko, M. A., Ekker, M., Wegner, J., Lin, W. and Westerfield, M. (1994). Combinatorial expression of three zebrafish genes related to *distal-less*: part of a homeobox gene code for the head. *J. Neurosci.* **14**, 3475-3486.

Allende, M. L. and Weinberg, E. S. (1994). The expression pattern of two zebrafish *achaete-scute* homolog (*ash*) genes is altered in the embryonic brain of the *cyclops* mutant. *Dev. Biol.* **166**, 509-530.

Amaya, E., Musci, T. J. and Kirschner, M. W. (1991). Expression of a dominant negative mutant of the FGF receptor disrupts mesoderm formation in Xenopus embryos. *Cell* **66**, 257-270.

Campuzano, S. and Modolell, J. (1992). Patterning of the *Drosophila* nervous system: the *achaete-scute* gene complex. *Trends Genet.* **8**, 202-208.

Christen, B. and Slack, J. M. (1999). Spatial response to fibroblast growth factor signalling in *Xenopus* embryos. *Development* **126**, 119-125.

Cobb, M. H. and Goldsmith, E. J. (1995). How MAP kinases are regulated. *J. Biol. Chem.* **270**, 14843-14846.

Crews, C. M., Alessandrini, A. and Erikson, R. L. (1992). The primary structure of MEK, a protein kinase that phosphorylates the *ERK* gene product. *Science* **258**, 478-480.

Deng, T. and Karin, M. (1994). c-Fos transcriptional activity stimulated by H-Ras-activated protein kinase distinct from JNK and ERK. *Nature* **371**, 171-175.

Ekker, M., Wegner, J., Akimenko, M. A. and Westerfield, M. (1992). Coordinate embryonic expression of three zebrafish *engrailed* genes. *Development* **116**, 1001-1010.

Fjose, A., Izpisua, B. J., Fromental, R. C. and Duboule, D. (1994). Expression of the zebrafish gene *hlx-1* in the prechordal plate and during CNS development. *Development* **120**, 71-81.

Fürthauer, M., Thisse, C. and Thisse, B. (1997). A role for FGF-8 in the dorsoventral patterning of the zebrafish gastrula. *Development* **124**, 4253-4264.

Gabay, L., Seger, R. and Shilo, B. Z. (1997a). In situ activation pattern of *Drosophila* EGF receptor pathway during development. *Science* **277**, 1103-1106.

Gabay, L., Seger, R. and Shilo, B. Z. (1997b). MAP kinase in situ activation atlas during *Drosophila* embryogenesis. *Development* **124**, 3535-3541.

Gotoh, Y. and Nishida, E. (1996). Signals for mesoderm induction. Roles of fibroblast growth factor (FGF)/mitogen-activated protein kinase (MAPK) pathway. *Biochim. Biophys. Acta* **1288**, F1-F7.

Hongo, I., Kengaku, M. and Okamoto, H. (1999). FGF signaling and the anterior neural induction in Xenopus. *Dev. Biol.* **216**, 561-581.

Houart, C., Westerfield, M. and Wilson, S. W. (1998). A small population of anterior cells patterns the forebrain during zebrafish gastrulation. *Nature* **391**, 788-792.

Inoue, A., Takahashi, M., Hatta, K., Hotta, Y. and Okamoto, H. (1994). Developmental regulation of islet-1 mRNA expression during neuronal differentiation in embryonic zebrafish. *Dev. Dyn.* **199**, 1-11.

Kimmel, C. B., Ballard, W. W., Kimmel, S. R., Ullmann, B. and Schilling, T. F. (1995). Stages of embryonic development of the zebrafish. *Dev. Dyn.* **203**, 253-310.

Klint, P. and Claesson-Welsh, L. (1999). Signal transduction by fibroblast growth factor receptors. *Front. Biosci.* **4**, D165-D177.

Koshida, S., Shinya, M., Mizuno, T., Kuroiwa, A. and Takeda, H. (1998). Initial anteroposterior pattern of the zebrafish central nervous system is determined by differential competence of the epiblast. *Development* **125**, 1957-1966.

Krauss, S., Concordet, J. P. and Ingham, P. W. (1993). A functionally conserved homolog of the Drosophila segment polarity gene *hh* is expressed in tissues with polarizing activity in zebrafish embryos. *Cell* **75**, 1431-1444.

Makita, R., Mizuno, T., Koshida, S., Kuroiwa, A. and Takeda, H. (1998). Zebrafish *wnt11*: pattern and regulation of the expression by the yolk cell and No tail activity. *Mech. Dev.* **71**, 165-176.

Maruoka, Y., Ohbayashi, N., Hoshikawa, M., Itoh, N., Hogan, B. L. M. and Furuta, Y. (1998). Comparison of the expression of three highly related genes, *Fgf8*, *Fgf17* and *Fgf18*, in the mouse embryo. *Mech. Dev.* **74**, 175-177.

Meyers, E. N., Lewandoski, M. and Martin, G. R. (1998). An *Fgf8* mutant allelic series generated by Cre- and Flp-mediated recombination. *Nat. Genet.* **18**, 136-141.

Mione, M., Shanmugalingam, S., Kimelman, D. and Griffin, K. (2001). Overlapping expression of zebrafish T-brain-1 and eomesodermin during forebrain development. *Mech. Dev.* **100**, 93-97.

Mohammadi, M., McMahon, G., Sun, L., Tang, C., Hirth, P., Yeh, B. K., Hubbard, S. R. and Schlessinger, J. (1997). Structures of the tyrosine kinase domain of fibroblast growth factor receptor in complex with inhibitors. *Science* **276**, 955-960.

Mori, H., Miyazaki, Y., Morita, T., Nitta, H. and Mishina, M. (1994). Different spatio-temporal expressions of three *otx* homeoprotein transcripts during zebrafish embryogenesis. *Mol. Brain Res.* **27**, 221-231.

Morita, T., Nitta, H., Kiyama, Y., Mori, H. and Mishina, M. (1995). Differential expression of two zebrafish *emx* homeoprotein mRNAs in the developing brain. *Neurosci. Lett.* **198**, 131-134.

Nasevicius, A. and Ekker, S. C. (2000). Effective targeted gene 'knockdown' in zebrafish. *Nat. Genet.* **26**, 216-220.

Ornitz, D. M. (2000). FGFs, heparan sulfate and FGFRs: complex interactions essential for development. *BioEssays* **22**, 108-112.

Reifers, F., Böhli, H., Walsh, E. C., Crossley, P. H., Stainier, D. Y. and Brand, M. (1998). *Fgf8* is mutated in zebrafish *acerebellar* (*ace*) mutants and is required for maintenance of midbrain-hindbrain boundary development and somitogenesis. *Development* **125**, 2381-2395.

Rohr, K. B., Barth, K. A., Vargam, Z. M. and Wilson, S. W. (2001). The Nodal pathway acts upstream of Hedgehog signaling to specify ventral telencephalic identity. *Neuron* **29**, 341-351.

Rubenstein, J. L., Shimamura, K., Martinez, S. and Puelles, L. (1998). Regionalization of the prosencephalic neural plate. *Annu. Rev. Neurosci.* **21**, 445-477.

Sakaguchi, T., Kuroiwa, A. and Takeda, H. (2001). A novel sox gene, 226D7, acts downstream of Nodal signaling to specify endoderm precursors in zebrafish. *Mech. Dev.* **107**, 25-38.

Schulte-Merker, S., Ho, R. K., Herrmann, B. G. and Nüsslein, V. C. (1992). The protein product of the zebrafish homologue of the mouse *T* gene is expressed in nuclei of the germ ring and the notochord of the early embryo. *Development* **116**, 1021-1032.

Shanmugalingam, S., Houart, C., Picker, A., Reifers, F., Macdonald, R., Barth, A., Griffin, K., Brand, M. and Wilson, S. W. (2000). Ace/Fgf8 is required for forebrain commissure formation and patterning of the telencephalon. *Development* **127**, 2549-2561.

Shimamura, K., Hartigan, D. J., Martinez, S., Puelles, L. and Rubenstein, J. L. (1995). Longitudinal organization of the anterior neural plate and neural tube. *Development* **121**, 3923-3933.

Shimamura, K. and Rubenstein, J. L. (1997). Inductive interactions direct early regionalization of the mouse forebrain. *Development* **124**, 2709-2718.

Shinya, M., Eschbach, C., Clark, M., Lehrach, H. and Furutani-Seiki, M. (2000). Zebrafish *dkk1*, induced by the pre-MBT wnt signaling, is secreted from the prechordal plate and patterns the anterior neural plate. *Mech Dev.* **98**, 3-17.

Stachel, S. E., Grunwald, D. J. and Myers, P. Z. (1993). Lithium perturbation and *goosecoid* expression identify a dorsal specification pathway in the pregastrula zebrafish. *Development* **117**, 1261-1274.

Toresson, H., Martinez-Barbera, J. P., Bardsley, A., Caubit, X. and Krauss, S. (1998). Conservation of *BF-1* expression in amphioxus and zebrafish suggests evolutionary ancestry of anterior cell types that contribute to the vertebrate telencephalon. *Dev. Genes Evol.* **208**, 431-439.

Whitlock, K. E. and Westerfield, M. (2000). The olfactory placodes of the zebrafish form by convergence of cellular fields at the edge of the neural plate. *Development* **127**, 3645-3653.

Wilson, S. W. and Rubenstein, J. L. R. (2000). Induction and dorsoventral patterning of the telencephalon. *Neuron* **28**, 641-651.

Woo, K. and Fraser, S. E. (1997). Specification of the zebrafish nervous system by nonaxial signals. *Science* **277**, 254-257.

Xu, J., Lawshé, A., MacArthur, C. A. and Ornitz, D. M. (1999). Genomic structure, mapping, activity and expression of fibroblast growth factor 17. *Mech. Dev.* **83**, 165-178.